# Conformation of the Acylation Site of Palmitoylgramicidin in Lipid Bilayers of Dimyristoylphosphatidylcholine†

Roger E. Koeppe, II,*,‡ T. C. Bas Vogt,§ Denise V. Greathouse,‡ J. Antoinette Killian,§ and Ben de Kruijff§

*Department of Chemistry and Biochemistry, University of Arkansas, Fayetteville, Arkansas 72701, and Department of Biochemistry of Membranes, Center for Biomembranes and Lipid Enzymology, Institute of Biomembranes, University of Utrecht, Padualaan 8, 3584 CH Utrecht, The Netherlands*

*Received August 28, 1995; Revised Manuscript Received January 16, 1996*⊗

ABSTRACT: Gramicidin A (gA) can be palmitoylated by means of an ester linkage to the OH group of the terminal ethanolamine that sits at the membrane−water interface in the functional gA channel. We have investigated palmitoyl-gA as a model transmembrane acylprotein. Ethanolamine-$d_4$ ($NH_2CD_2CD_2OH$) was incorporated into gA by total synthesis, and a portion of the labeled gA was palmitoylated. Solid-state $^2$H-NMR spectra of acyl- and nonacyl-gA in hydrated dimyristoylphosphatidylcholine (DMPC) bilayers were compared. The spectra for both oriented and nonoriented samples at 4 and at 40 °C indicate that the ethanolamine of gA is highly mobile prior to acylation, but essentially immobile after palmitoylation. The $^2$H quadrupolar splittings allow the conformation of the ethanolamine group in acyl-gA to be determined. By combining our data with the previously determined quadrupolar splittings for deuterium labels on the palmitoyl chain [Vogt, T. C. B., Killian, J. A, & de Kruijff, B. (1994) *Biochemistry 33*, 2063−2070], we also propose a model for the acyl chain. The ethanolamine group rotates over Leu$^{10}$ and toward the outside of the gA channel's cylinder upon acylation, so that the attached acyl chain passes between the side chains of Trp$^9$ and Leu$^{10}$. To accommodate the acyl chain, the six-membered portion of the indole ring of Trp$^9$ is displaced by about 0.9 Å, by means of 1−2° rotations in $\chi_1$ and $\chi_2$.

The attachment of palmitic acid to a protein via an ester or thio ester linkage is one of several ways that a protein may be covalently modified by lipids. Diverse groups of proteins have been found to be palmitoylated, including viral proteins (Rose et al., 1984; Bonatti et al., 1989; Veit et al., 1991; Veit & Schmidt, 1993), and integral membrane proteins such as the transferrin receptor (Jing & Trowbridge, 1990), the $\beta$2-adrenergic receptor (O'Dowd et al., 1989), cell surface glycoprotein CD4 (Crise & Rose, 1992), rhodopsin (Papac et al., 1992), the membrane-bound form of acetylcholinesterase (Randall, 1994), endoplasmic reticulum protein p63 (Schweizer et al., 1995), and G protein α subunits (Wilson & Bourne, 1995). In most cases, little is known about the structure or function of the covalently attached palmitate. Possible functions include promotion of the binding of the acylated protein to a cell membrane or modulation of the conformation or interactions of an intrinsic membrane protein.

Several studies have been done on the location and accessibility of palmitoyl groups attached to transmembrane proteins. Vogt et al. (1994), using deuterated palmitoyl chains attached to the ethanolamine group of gramicidin, determined that the portion of the acyl chain near the site of covalent attachment to the peptide is immobilized, whereas the more distal part of the chain behaves in a manner similar to that of free fatty acids in bilayers. Favre et al. (1979) reached a qualitatively similar conclusion using spin-labeled fatty acids attached to cysteines in rhodopsin. Moench et al. (1994) attached fluorescent fatty acid labels to the cysteine palmitoylation sites in rhodopsin and determined that, again, the labels are situated in the membrane much as free fatty acids.

We have further investigated the effects of palmitoylation upon gramicidin (gA[1] ), a functional cation channel that serves as a model for an intrinsic membrane protein. Gramicidin is an attractive model for studies of acylation because both structure and function can be examined at high resolution in this system. Changes in structure and function that are induced by acylation can therefore be correlated.

The structure of the gA channel in a membrane is a right-handed, *N*-formyl-to-*N*-formyl, single-stranded $\beta^{6.3}$-helical dimer, which is known from two-dimensional NMR spectroscopy in aqueous SDS (Arsen'ev et al., 1985, 1986) and solid-state $^2$H NMR in hydrated DMPC (Ketchem et al., 1993). The channel structure correlates well with a characteristic CD spectrum that has positive peaks at 218 and 235 nm (Wallace et al., 1981; Killian et al., 1988; Greathouse et al., 1994). The molecularity of two for the channel is known from fluorescence (Veatch & Stryer, 1977), size exclusion chromatography (Bañó et al., 1992), and hybrid channel analysis (Cifu et al., 1992; Koeppe et al., 1992). The backbone conformations of sequence analogue channels can be referenced to known structures through hybrid channel analysis (Durkin et al., 1990, 1993).

† This work was supported in part by NIH Grant GM34968 from the U.S. Public Health Service and NSF Grant EHR-9108762.

* Address correspondence to Roger E. Koeppe II.

‡ University of Arkansas.

§ University of Utrecht.

⊗ Abstract published in *Advance ACS Abstracts,* March 1, 1996.

[1] Abbreviations: gA, gramicidin A; SDS, sodium dodecyl sulfate; DMPC, dimyristoylphosphatidylcholine; CD, circular dichroism; NMR, nuclear magnetic resonance; HPLC, high-performance liquid chromatography.

0006-2960/96/0435-3641$12.00/0 

When gA is palmitoylated, the acyl chain is attached to the C-terminal ethanolamine[2] blocking group. The backbone structure of acyl-gA is similar to that of native (nonacylated) gA, as shown by CD spectoscopy (Vogt et al., 1991), hybrid channel analysis (Koeppe et al., 1992; Williams et al., 1992), and NMR spectroscopy (Koeppe et al., 1995). While the backbone structures of acyl-gA and gA are similar, the side chains of $Trp^9$ and $Leu^{10}$ are perturbed by acylation, as shown by $^1$H- and $^2$H-NMR (Koeppe et al., 1995). The single-channel conductance is unaffected by acylation, but the average channel lifetime is increased 5-fold (Koeppe et al., 1985; Williams et al., 1992; Vogt et al., 1992).

To further examine the structure of acyl-gA, we have deuterated the C-terminal ethanolamine and have used solid-state $^2$H-NMR spectroscopy to assess changes in the mobility and orientation of the ethanolamine moiety upon acylation. By combining our results with those of Vogt et al. (1994) for palmitoyl-$^2$H-labeled acyl-gA, we were able to construct a molecular model for the ethanolamine and acyl chain in acyl-gA. The model demands a movement of the $Trp^9$ indole away from $Leu^{10}$ upon acylation, as has been independently demonstrated using $^2$H-labeled side chains (Koeppe et al., 1995). Structural changes such as side chain movements, and a slowing of the motion of the ethanolamine itself, may relate to functional changes such as the increased average lifetime for acyl-gA channels.

## MATERIALS AND METHODS

Ethanolamine-$d_4$ was obtained from Cambridge Isotope Laboratories (Andover, MA) and from Isotec (Miamisburg, OH). gA was synthesized as previously described (Becker et al., 1991; Koeppe et al., 1992, 1994a, 1995) and was cleaved from the 1% divinylbenzene Wang resin (Advanced Chemtech, Louisville, KY) using 1 mL of ethanolamine-$d_4$ in 5 mL of dimethylformamide at 70 °C for 24 h. The resin was removed by filtration, and the product was precipitated by the addition of water, collected by centrifugation, resuspended, and reprecipitated. The resulting labeled gA gave a single peak by analytical HPLC (Koeppe & Weiss, 1981) and was used without further purification.

Fifty milligrams of the ethanolamine-$d_4$-labeled gA was acylated by the procedure of Vogt et al. (1991), and a new purification procedure was used. The 2 mL reaction mixture was diluted with 4 mL of methanol and injected onto a 1.5 cm diameter by a 200 cm long column of Sephadex LH-20 (Pharmacia-LKB, obtained from Sigma Chemical Co., St. Louis, MO). The column was pumped at 0.45 mL/min (∼2−6 psi, 20−25 °C), and materials eluted in the following volumes: acyl-gA, 140 mL; gA, 145 mL; palmitic acid, 200 mL; and 4-pyrolidinopyridine and other excess starting reagents, 260 mL. The acyl-gA-$d_4$ thus obtained gave a single peak by octylsilica reversed-phase HPLC (Koeppe et al., 1985) and the expected *m/z* of 2122 for $C_{115}H_{166}D_4N_{20}O_{18}$ by electrospray mass spectrometry (Mass Consortium Corp., San Diego, CA).

Glass plates, 4.8 × 23.0 mm, thickness no. 00 (0.06−0.08 mm) were from Marienfeld Laboratory Glassware (Bad Mergentheim, Germany). DMPC was from Avanti Polar Lipids (Alabaster, AL). All other materials were as in Koeppe et al. (1995). Oriented samples on glass plates were prepared as described (Killian et al., 1992), by resuspending in chloroform (0.8 mL) a dried film of 6 $\mu$mol of labeled gA or acyl-gA and 60 $\mu$mol of DMPC, applying the sample evenly to 50 glass plates, drying extensively, stacking the plates in a glass cuvette, hydrating with 38 $\mu$L of $^2$H-depleted $H_2O$, sealing the container, and incubating a minimum of 72 h at 40 °C.

Nonoriented samples were prepared by suspending a dried film of 6 $\mu$mol gA-$d_4$ or acyl-gA-$d_4$ and 60 $\mu$mol of DMPC in excess $^2$H-depleted $H_2O$, centrifuging for 2 h (40 °C) in a 7.5 mm diameter glass tube at 14600*g*, removing excess water, and breaking the tube to a length of 3 cm prior to sealing.

$^2$H-NMR spectra were recorded as previously (Koeppe et al., 1994a, 1995), using a Bruker MSL 300 spectrometer, and these parameters: a 4 $\mu$s 90° pulse, a 100 ms interpulse time, 0.5−1.5 million scans, and a 60 $\mu$s echo delay time. The signal-to-noise ratio was increased by application of a line broadening of 200 Hz prior to Fourier transformation for spectra of the oriented samples, or 1 kHz (gA) or 3 kHz (acyl-gA) for the nonoriented sample spectra. Molecular modeling to fit the geometry of the acyl-ethanolamine moiety to the observed quadrupolar splittings was accomplished as described in Koeppe et al. (1994a), using a C−D quadrupolar coupling constant, $e^2qQ/h$, of 168 kHz multiplied by 0.92 to account for small-amplitude (whole-molecule) motional averaging (Killian et al., 1992; Prosser et al., 1994). Models were visualized using the program InsightII (Biosym. Technologies, San Diego, CA). The relative energies of different models were compared and/or minimized using the conjugate gradient option of the program Discover (Biosym.).

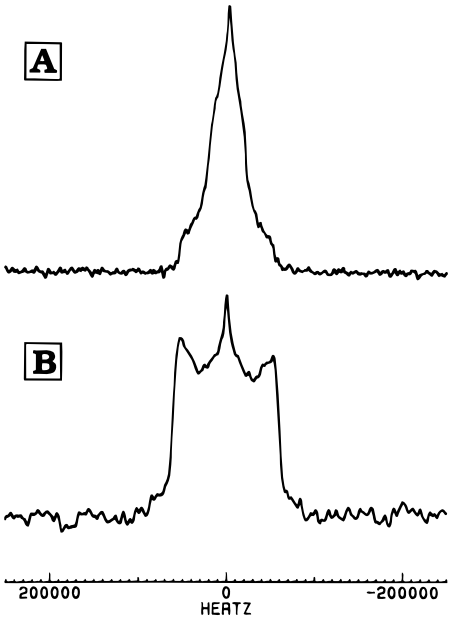


FIGURE 1: $^2$H-NMR spectra before and after palmitoylation for nonoriented samples of ethanolamine-$d_4$-gA in DMPC bilayers at 4 °C: (A) gA and (B) palmitoyl-gA.

## RESULTS

*Nonoriented Samples*. Figure 1 compares the powder pattern spectra of ethanolamine-$d_4$-gA and -acyl-gA in

[2] The C-terminal group of gA would be more properly termed "aminoethanol" or "amidoethanol" to indicate the presence of the free hydroxyl group, to which the acyl chain is esterified in acyl-gA, but we continue to use the traditional term "ethanolamine", which is pervasive in the literature.

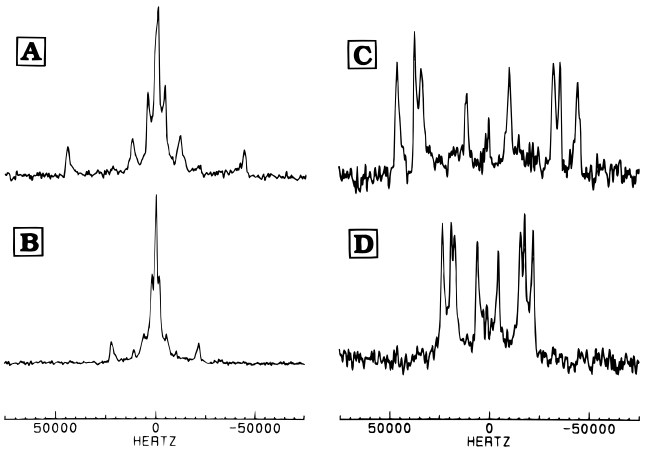


FIGURE 2: $^2$H-NMR spectra before and after palmitoylation for ethanolamine-$d_4$-gA in DMPC bilayers oriented at a temperature of 40 °C: (A) gA oriented at $\beta = 0°$, (B) gA at $\beta = 90°$, (C) palmitoyl-gA at $\beta = 0°$, and (D) palmitoyl-gA at $\beta = 90°$.

hydrated DMPC bilayers at 4 °C. At this low temperature, the global rotational motion of the gramicidin about its helix axis is slowed to a correlation time of >1.3 s (Cornell et al., 1988; Lee & Cross, 1994), so that the possibility of local motion can be tested (Lee & Cross, 1994; Lee et al., 1995). With the long-axis whole-molecule rotation slowed due to the low temperature, the only motional averaging that can occur is that due to local motions. If there were no such local motions, then a Pake pattern would be expected with full quadrupolar splitting. Instead, for the ethanolamine of gA, two spectral components are evident in Figure 1A, with line widths at half-height of approximately 40 and 106 kHz. These components probably represent the two distinct $CD_2$ groups of the ethanolamine; the spectrum suggests that there are large-amplitude motions for at least one of the $CD_2$ groups, probably the outer one.

The powder pattern spectrum of ethanolamine-$d_4$-acyl-gA at 4 °C is very different from that of gA. After acylation, a distinct Pake pattern is seen (Figure 1B), with a quadrupolar splitting of 108 kHz. This indicates a greatly *reduced mobility* for the ethanolamine group when the palmitoyl chain is attached (the intensity near the middle of Figure 1B is most likely due to residual deuterium from the lipids or water). The reduced mobility is likely due to a "tethering" of the ethanolamine by the covalent attachment of the acyl chain; following acylation, the ethanolamine is no longer the terminal group on the chain.

*Oriented Samples*. The $^2$H-NMR spectra were also recorded for oriented samples of acylated and nonacylated ethanolamine-$d_4$-gA in (hydrated) DMPC (Figure 2). For gA oriented with $\beta = 0°$, four peaks with $\Delta\nu_q$ of 88.3, 23.9, 8.5, and <1.3 kHz are observed for the four deuterons of the ethanolamine-$d_4$ group (Figure 2A). When the gA sample is turned to the $\beta = 90°$ orientation, there is a 2-fold reduction in each $\Delta\nu_q$ (Figure 2B), due to rapid axial reorientation of the gramicidin about its long axis (Nicholson et al., 1987; Cornell et al., 1988; Killian et al., 1992). Also in the $\beta = 90°$ orientation, a minor peak becomes evident (corresponding to a $\Delta\nu_q$ of 43.7 kHz at $\beta = 0°$); the meaning of this peak is unknown. Because the ethanolamine in gA is highly mobile (concluded from Figure 1A), it is not feasible to relate these $\Delta\nu_q$ values to the orientations of C−D bonds in ethanolamine-labeled gA.

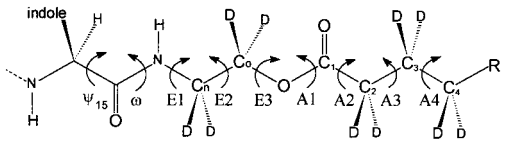


FIGURE 3: Torsion angles that define the conformation of the ethanolamine and of carbons 1−4 of the acyl chain in acyl-gA. In this work, carbons Cn and Co have been labeled; carbons C2, C3, and C4 and others in the palmitoyl chain were labeled by Vogt et al. (1994).

For ethanolamine-labeled acyl-gA, the $^2$H-NMR peaks appear at $\Delta\nu_q$ values of 21.1, 65.9, 72.4, and 89.9 kHz (Figure 2C), i.e. at different and generally larger $\Delta\nu_q$ values than for the nonacylated sample. Again, the quadrupolar splittings are 2-fold reduced when the acyl-gA sample is turned 90° (Figure 2D), indicating that axial reorientation for acyl-gA, as well as for gA, is fast on the NMR time scale. The larger $\Delta\nu_q$ values are consistent with a reduction in large-amplitude local motion for the ethanolamine after acylation, as was also indicated by Figure 1B. Furthermore, the data of Vogt et al. (1994), in which distinct peaks with unique $\Delta\nu_q$ values are seen for each member of each pair of deuterons on C2, C3, and C4 of labeled palmitoyl chains in acyl-gA, suggest that the C1−C4 portion of the attached palmitoyl chain is much less mobile than the distal part of the acyl chain and does not undergo large-amplitude local motion. Together, the $^2$H-NMR data for ethanolamine-labeled samples (Figures 1B and 2C,D) and acyl chain-labeled samples (Vogt et al., 1994) suggest that one can construct a model for the orientation and geometry of a fixed ethanolamine group in acyl-gA, which does not exhibit large-amplitude local motion.

The quadrupolar splittings ($\Delta\nu_q$) are related to the C−D bond orientations[3] by

$$\Delta\nu_q = {}^3/_2 e^2qQ/h[{}^1/_2(3\cos^2\Theta - 1)][{}^1/_2(3\cos^2\beta - 1)] \quad (1)$$

where $e^2qQ/h$ is the C−D quadrupolar coupling constant, $\Theta$ is the angle between a C−D bond and the channel axis, and $\beta$ is the angle between the membrane normal and the magnetic field, $H_o$. For modeling the ethanolamine group (see the diagram in Figure 3), the orientations of each of the $C_n$−D and $C_o$−D values were fit to the $\Delta\nu_q$ values of magnitude 21.1, 65.9, 72.4, and 89.9 kHz for ethanolamine-$d_4$-acyl-gA by rotation about bonds E1 and E2 (Figure 3). Values of 132° for angle $\Psi_{15}$ (Figure 3) and 179° for angle $\omega$ were taken from the model of Killian et al. (1992). The value of $\Psi_{15}$ is immaterial here, because conformational solutions are expressed in terms of the sum ($\Psi_{15}$ + E1). The planar peptide unit maintains $\omega$ near 180°.

Torsion angles E1 and E2 (Figure 3) were searched together by the procedure of Koeppe et al. (1994), in 1° intervals for each angle, using the ethanolamine-$d_4$ data for oriented palmitoylgramicidin in DMPC at 40 °C, with no prior assumptions about the signs or assignments of the quadrupolar splittings. Pairs of solutions are related by 180° around the N−$C_n$ bond (see Figure 4, in which d specifies

[3] The equivalent deuterium labels on the two antiparallel subunits in an oriented gramicidin channel dimer will give rise to the same quadrupolar splittings, because C−D bond orientations of $\Theta$ and 180° − $\Theta$ correspond to the same value of $\Delta\nu_q$.

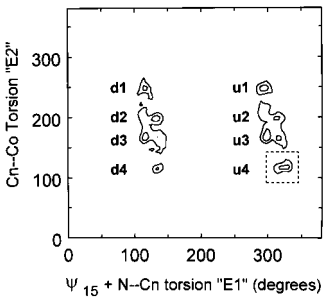


FIGURE 4: Conformation of the ethanolamine group in palmitoyl-gA. The boxed contour indicates the most probable conformation that is consistent with the $^2$H quadrupolar splittings and the molecular model of the gA backbone. The contours are drawn in intervals of 0.04 deg$^{-2}$ in 1/sumsq, according to eq 2 of Koeppe et al. (1994a) for the analysis of the $^2$H quadrupolar splittings.

Table 1: Steric Hindrance of Ethanolamine Rotamers with a Covalently Attached 2-Carbon Acyl Chain

| orientation[a] | excess energy (calculated by Discover) |
|---|---|
| up | |
| u1 | 23 kcal/mol |
| u2 | 0[b] |
| u3 | 20 kcal/mol |
| u4 | 0 |
| down | |
| d1 | 44 kcal/mol |
| d2 | [c] |
| d3 | [c] |
| d4 | [c] |

[a] Orientations from Figure 4. [b] The u2 orientation interferes with an acyl chain that is longer than two carbons. [c] Indicates no convergence.

ethanolamine down, or toward the bilayer center, and u means ethanolamine up, or toward the membrane−solution interface).

Possible solutions in Figure 4 were tested for steric interference with a 2-carbon acetyl derivative on the ethanolamine using the program Discover. This test showed that the d solutions and two of the u solutions would not accommodate an attached acyl chain without steric interference with the rest of gA, as shown by the high energies in Table 1. For three of the d solutions, the steric conflict was so severe that refinement was not possible. Consideration of a longer acyl chain eliminated solution u2, leaving u4 as the only plausible solution (small box in Figure 4).

Figure 5 shows a helical wheel diagram to illustrate the conformation of the ethanolamine of acyl-gA that corresponds to solution u4 (solid line; E1 of 184° and E2 of 114°). For comparison, the dotted line in Figure 5 shows a probable average orientation for the highly mobile ethanolamine of nonacyl-gA, proposed by Arsen'ev et al. (1986) and allowing a hydrogen bond to the carbonyl of Leu$^{10}$.

Next, consideration was given to the ester linkage and the acyl chain itself. Torsions E3 and A1 (Figure 3) are not directly accessible from the deuterium NMR data. Ester "resonance", although less strong than amide "resonance", nevertheless restricts the rotation about bond A1. Further, the *Z* (Zusammen) orientation is favored by about 9 kcal/mol over an *E* (Entgegen) conformation (Wiberg & Laidig, 1987). The *Z* conformation is defined when E3 and A1 are both 180°, in "peptide standard" nomenclature, i.e. C−C−O−C for E3 and C−O−C−C for A1 (both "along the chain"

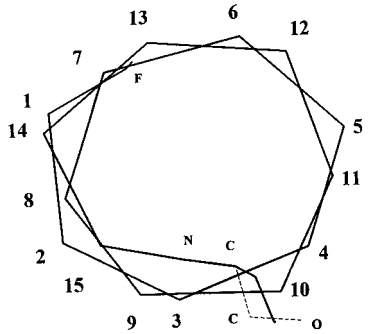


FIGURE 5: Model (helical wheel diagram) to illustrate the change in the conformation of the ethanolamine of gA upon acylation. The backbone and ethanolamine for acyl-gA are shown by the solid lines. The dashed segments show one of several interconverting conformations for the ethanolamine of nonacyl-gA, this one allowing a hydrogen bond to the carbonyl of Leu$^{10}$ (see text): Cα carbons, numbered; formyl group, F; ethanolamine, N−C−C−O.

in Figure 3). The *Z* conformation was found to allow subsequent modeling of the acyl chain (see below) to proceed nicely.[4]

For the *Z* ester conformation, the $\Delta\nu_q$ values for [2,2-$^2$H]-palmitoyl-gA (5.0 and 18.0 kHz; Vogt et al., 1994) were used to define torsion angle A2. The search yielded two closely spaced solutions for A2 at 12 or 21°. These solutions were so close to each other that either of them could be used for subsequent modeling (with equivalent results). The A2 solutions were highly favored, with sums of squared deviations (Koeppe et al., 1994a) 2 orders of magnitude lower than any other solutions (data not shown). With A2 fixed at 21° (or 12°), a search using the quadrupolar splittings due to deuterons on C3 and C4 of palmitoyl-gA yielded a unique solution with both A3 and A4 very near 180° (graph not shown). This completed the determination of the seven torsion angles E1, E2, E3, and A1−A4 (Figure 3).

For consideration of the rest of the palmitoyl chain, we made use of the previous findings of Vogt et al. (1994) that the acyl chain bends in the vicinity of C5−C7 and that the remainder of the chain is highly mobile. To position the C8−C16 portion of the chain near the exterior hydrophobic surface of gramicidin (for favorable "packing"), it was found that torsions C4−C5 and C6−C7 should both be near −80°, in agreement with the bend predicted by Vogt et al. (1994). The remainder of the palmitoyl chain, although known to be mobile, was modeled as extended chain. In this model, the acyl chain bends over Leu$^{10}$ and attempts to pass between the side chains of Leu$^{10}$ and Trp$^9$. The initial energy (program Discover) for the structure was 5 000 000 kcal/mol, primarily due to steric interference between the acyl chain and Trp$^9$, and to a lesser extent Leu$^{10}$. Nevertheless, the structure refined quickly, with small adjustments to the acyl chain and Leu$^{10}$ and a 0.9 Å movement of the ring of Trp$^9$ away from the acyl chain (see Discussion).

Table 2 shows a comparison of the final bond orientations in the refined model with the predictions of the $\Delta\nu_q$ values from the $^2$H-NMR spectra. The largest deviation between model and experiment is 4.0°, and the average deviation is 1.6° (Table 2). The model for acyl-gA therefore agrees very well with the $^2$H-NMR data.

[4] Other possible values were also tried, but 180° assignments for E3 and A1 were found to give the best fits to the early part of the acyl chain in the subsequent modeling steps.

Table 2: Predicted and Observed $^2$H Bond Orientations in Labeled Acyl-gA for the Condition of No Large-Amplitude Local Motion[a]

| | angle with respect to $H_o$ (deg) | | | |
|---|---|---|---|---|
| bond[c] | model | NMR | deviation | $\Delta\nu_q$[b] ($\beta = 0°$) |
| $C_n$−D | 51.7 | 51.1 | 0.6 | 21.1 |
| −D | 68.8 | 69.3 | −0.5 | −72.4 |
| $C_o$−D | 78.2 | 74.2 | 4.0 | −89.9 |
| −D | 46.3 | 43.7 | 2.6 | 65.9 |
| C2−D | 51.2 | 53.0 | −1.8 | 10.0 |
| −D | 59.9 | 61.4 | −1.5 | −36.0 |
| C3−D | 57.9 | 56.9 | 1.0 | −12.4 |
| −D | 54.3 | 55.0 | −0.7 | −1.6 |
| C4−D | 54.8 | 55.5 | −0.7 | −4.6 |
| −D | 55.4 | 57.8 | −2.4 | −17.4 |

[a] The torsion angles E1, E2, E3, A1, A2, A3, and A4 for the bonds are defined in Figure 3. A small-amplitude ("librational") "motion" parameter of 0.92 has been applied to the C−D quadrupolar coupling constant of 168 kHz throughout [see Killian et al. (1992) and Prosser et al. (1994)]. [b] Quadrupolar splitting observed in Figure 2C ($C_n$−D and $C_o$−D) and in Vogt et al. (1994) (C2−D, C3−D, and C4−D), with $\beta = 0°$ and sign determined as in Koeppe et al. (1994a). [c] See Figure 3 for the bond definitions.

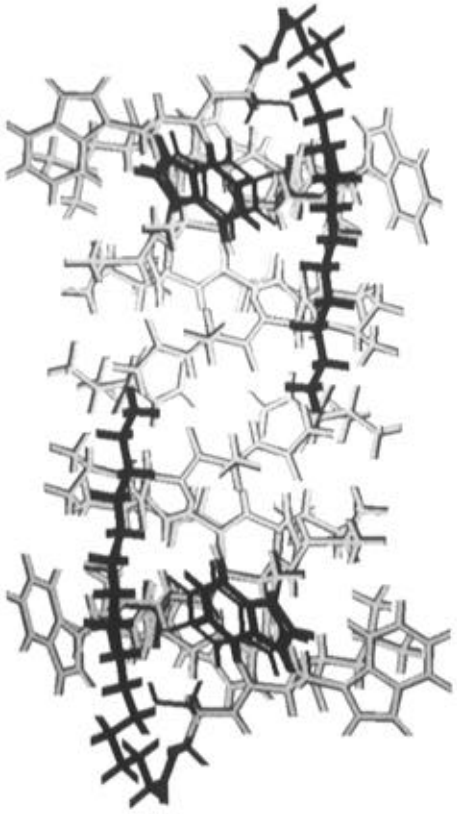

FIGURE 6: Superposition of wire models for acyl-gA and gA. Carbons 1−5 of the palmitoyl chain conform to the $^2$H-NMR data, while carbons 6−16 are depicted as a bend followed by an extended chain that represents a snapshot view of a highly mobile structure (see text). The significant differences in the models appear bold: (i) The acyl chain is new, and the ethanolamine has moved to bond to it. (ii) The side chains of Trp$^9$ and Leu$^{10}$ are forced to reorient due to steric interference with the acyl chain.

Figure 6 shows a superposition to compare the wire models for acyl-gA and gA. The underlying gA model in Figure 6 is that of Arsen'ev et al. (1986), as energy minimized by Killian et al. (1992), with Trp$^9$ initially in the orientation of Figure 7A of Koeppe et al. (1994a), consistent with $^2$H-NMR spectra for [ring-$^2$H-Trp$^9$]gA. The lighter, nonbold, majority of the structure in Figure 6 is identical in gA and acyl-gA. The significant differences in the models are highlighted bold in Figure 6. These include (i) a rotation of the ethanolamine group to form the ester bond with the acyl chain, (ii) the introduction of the new acyl chain, and (iii) a movement of Trp$^9$ away from Leu$^{10}$ to accommodate the acyl chain. The last effect has been predicted on the basis of $^1$H- and $^2$H-NMR spectra of Trp$^9$ and Leu$^{10}$ in gA and acyl-gA (Koeppe et al., 1995).

## DISCUSSION

When the acylgramicidins were discovered (Koeppe et al., 1985), an ester attachment of a fatty acid to the terminal ethanolamine of gramicidin was inferred from NMR spectroscopy. The ester bond has since been verified by chemical synthesis (Vogt et al., 1991) and mild alkaline hydrolysis (Williams et al., 1992). Among the fatty acids found in natural acylgramicidins are palmitic and stearic acids and pentadecanoic and 12-methyltetradecanoic acids (Williams et al., 1992). In this paper, we have characterized the ethanolamine−acyl chain linkage by examining synthetic gA and palmitoyl-gA which were deuterated on both carbons of the ethanolamine. The $^2$H-NMR spectra have revealed that the ethanolamine is mobile prior to acylation and have led to a model for the ethanolamine and the acyl chain in palmitoyl-gA. The general features of the model may be expected to apply to other acylproteins in biological membranes. Following a discussion of the specific results for gramicidin, we will consider briefly the general issues.

*Dynamics of the Ethanolamine of Gramicidin*. The membrane-buried *N*-formyl and water-exposed *C*-ethanolamine blocking groups of gA mask the charges that would be present at the ends of the free peptide. Additional functions to aid ion binding or ion transport have been proposed for the ethanolamine group, but these have been largely discounted by experiment. For example, neither the removal of the terminal $CH_2OH$ nor its esterification alters the gramicidin single-channel conductance for $Na^+$ ions (Trudelle et al., 1987; Williams et al., 1992; Vogt et al., 1992).

Information on the precise configuration of the ethanolamine tail of gA has been elusive (Pullman, 1987). Several models of the gA channel have included hydrogen bonds from the ethanolamine OH to the peptide backbone (Pullman & Etchebest, 1983; Arsen'ev et al., 1986; Koeppe et al., 1994b). For a right-handed $\beta^{6.3}$-helical (single-stranded) structure, the established structure for the gA channel (Arsen'ev et al., 1986; Ketchem et al., 1993), such a hydrogen bond would link the ethanolamine hydroxyl to the backbone carbonyl oxygen of Leu$^{10}$ (Arsen'ev et al., 1986). Although the hydrogen bond is appealing in the model (Figure 5), support for the concept of breaking the hydrogen bond and allowing a flexible ethanolamine tail has come from calculations (Etchebest & Pullman, 1984; Etchebest et al., 1985) and from the refinement of $^1$H-NMR data for gA in SDS (Lomize et al., 1992).

The $^2$H-NMR data for (nonacyl) gA favor a mobile ethanolamine (Figure 1A) that could be in the hydrogen-bonded configuration only transiently. In the dotted segments of Figure 5, we project the position of a hydrogen-bonded ethanolamine, purely for purposes of illustration, because the other states that are dynamically sampled cannot be unequivocally determined using the available data.

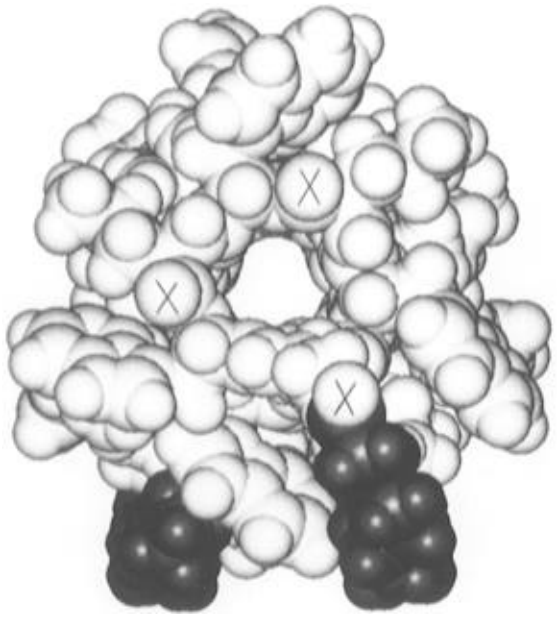

FIGURE 7: End view of a space-filling model of an acyl-gA channel dimer, with the amino acids shown light and the acyl chains dark. The conformation is the same as that depicted in Figure 6. The acyl chain on the left is coming from the distal subunit and is radially <40° away from the proximal acyl chain. The ester carbonyl oxygen (marked with ×) is available, along with those of $Leu^{12}$ and $Leu^{14}$, to help coordinate an incoming ion.

Upon acylation, the ethanolamine assumes a fixed conformation (Figure 5, solid segments) that is different from the putative hydrogen-bonded conformation. The $^2$H-NMR data have allowed us to define this ethanolamine conformation and that of C1−C5 of the acyl chain, under the condition that C1−C4 of the acyl chain adopt a rigid structure. Although we do not have unambiguous proof for this, there are four arguments that favor a highly immobile structure for the upper part of the acyl chain [after Vogt et al. (1994)]. (i) The $^2$H signals from the C2−C4 region of the chain exhibit low intensity, which is attributed to fast $T_2$ relaxation. (ii) The same $^2$H signals exhibit very short $T_1$ values. (iii) Double quadrupolar splittings have been assigned for deuterons at C2 and C3 and inferred for deuterons at C4. (iv) The calculated torsion angles in both the earlier models (Vogt et al., 1994) and the present model (Figures 6 and 7, Table 2) are close to 180°, for the *trans* portion of the chain, or −60°, for the bend in the chain (C4−C5 and C6−C7 bonds).

*Conformation and Influence of the Attached Acyl Chain.* The covalent acyl chain can be accommodated easily by the transmembrane gA molecule. The results from the molecular modeling (Figure 6) suggest that there are no long-range or broad effects on the conformation of the polypeptide, but rather only local effects, in agreement with previous $^2$H-NMR results for selectively deuterated side chain and backbone groups in gA and acyl-gA (Koeppe et al., 1995). The largest local effects that are indicated by the modeling involve the indole ring of $Trp^9$.

In Table 3, we compare some steric parameters for $Trp^9$ before and after acylation. The numbers in Table 3 correspond to the shift in ring orientation that is shown in Figure 6. The minimum necessary change in the orientation of $Trp^9$ to make room for the acyl chain is small, yet significant: 1.7° in $\chi_1$ and 0.9° in $\chi_2$. The corresponding changes in the C−H bond orientations range from 2 to 4°, and the displacements of the ring carbon atoms are small, all <1 Å

Table 3: Movement of $Trp^9$ To Accommodate the Acyl Chain in Palmitoylgramicidin[a]

| $Trp^9$ carbon atom | change in C atom position (Å) | change in C−H bond orientation (deg) |
|---|---|---|
| Cδ1 | 0.34 | 3.4 |
| Cε3 | 0.53 | 2.1 |
| Cζ3 | 0.82 | 2.5 |
| Cη2 | 0.96 | 2.3 |
| Cζ2 | 0.83 | 4.4 |
| torsion angle | | change (deg) |
| $\chi_1$ | | 1.7 |
| $\chi_2$ | | 0.9 |

[a] The parameters are derived from the differences in the $Trp^9$ coordinates in the molecular models of gA and acyl-gA depicted in Figure 6. The initial $Trp^9$ position in gA was that described in Figure 7A of Koeppe et al. (1994a). The change in the angle between the plane of the indole ring and the channel axis following acylation was 4.2°.

(Table 3). If $Trp^9$ should move to another region of conformational space, still consistent with the $^2$H-NMR spectra, then the ring movement upon acylation would be much larger than the minimal values discussed here [see Hu et al. (1993), Koeppe et al. (1994a, 1995), and Hu et al. (1995)].

In this paper, the conclusion about the movement of $Trp^9$ to accommodate the acyl chain is based purely on the refinement of a model derived from the $^2$H-NMR spectra for deuterium labels on the ethanolamine and on the palmitoyl chain. A similar conclusion has also been reached by examination of $^2$H-NMR spectra for labeled acyl- and nonacyl-[d5-$Trp^9$]gA (Koeppe et al., 1995). It is interesting to note that both the molecular modeling (Figure 6) and the $^2$H-NMR spectra for [d5-$Trp^9$]gA (Koeppe et al., 1995) predict changes of 2−4° in the orientations of ring C−D bonds. The model in Figure 6 is also consistent with the suggestions of Vogt et al. (1994) that the acyl chain should pass over $Leu^{10}$ and should bend in the "motional transition region" of C5−C6.

*Implications for Channel Function.* The significant functional characteristics of acyl-gA are a single-channel conductance identical to that of gA for alkali cations, a 5-fold longer average single-channel duration, and a decreased channel-forming potency (Koeppe et al., 1985; Williams et al., 1992; Vogt et al., 1992). The reduced channel-forming potency of acyl-gA is an elusive property, but it may relate to differences between acyl-gA and gA in the kinetics of refolding (O'Connell et al., 1990; Zhang et al., 1992; Abdul-Manan & Hinton, 1994) that should accompany surface association, membrane entry, and channel formation [see Williams et al. (1992) and Vogt et al. (1992)].

The 5-fold increase in average channel duration is small in energetic terms, yet easily measurable. The increased dimer stability is perhaps related to a favorable packing of the covalent acyl chains between the amino acid side chains and the membrane lipids, as suggested by Figure 6 and by the corresponding end view of acyl-gA in Figure 7. The mechanism of channel closing could initiate with an unfolding of one monomer (e.g. from the C-terminal ethanolamine) or with an independent twisting (long-axis rotation) of the two monomers relative to each other. In the former case, the acyl chain may help (slightly) to stabilize the C-terminal, including the tryptophans at the membrane−water interface,

and thereby inhibit monomer unfolding. Regarding the long-axis rotation, comparisons of $^2$H-NMR spectra for $\beta = 0°$ and $\beta = 90°$ orientations of side chain-labeled acyl-gA's in hydrated DMPC show that, as for gA, the overall rate of rotation of the acyl-gA channel about its long axis remains rapid for temperatures above the lipid phase transition temperature (Koeppe et al., 1995). This feature has also been demonstrated for the ethanolamine-$d_4$-labeled samples used for this paper (Figure 2). From Figure 7, it is evident that the two palmitoyl chains slightly increase the radius of the channel exterior (overall "girth"). The chains lie along the same side of the acyl-gA cylinder and are separated by $<40°$ in the radial dimension (Figure 7). Although the chains do not interfere greatly with long-axis rotation of the dimer, independent motions of the monomers could be inhibited slightly, thus slowing dissociation.

A cation coming into the gA channel is coordinated initially by the carbonyl oxygens of Leu$^{12}$ and Leu$^{14}$, and possibly of Leu$^{10}$ (Smith et al., 1990). The former are unobscured by the acyl chain, but the latter is covered by the ethanolamine and the acyl chain in acyl-gA (Figure 7). However, the acyl ester contributes a new carbonyl function that is situated directly above the Leu$^{10}$ carbonyl and 6 Å farther out toward the aqueous solution (4 Å farther out than the Leu$^{14}$ carbonyl, Figure 7). The acyl ester could therefore partially substitute for the function of the Leu$^{10}$ carbonyl in ion entry and initial ion coordination. Whatever the case, the single-channel conductance for $Na^+$ or $Cs^+$ is not affected by acylation (Koeppe et al., 1985; Williams et al., 1992; Vogt et al., 1992).

*Implications for Acylproteins in Membranes.* This paper and those of Vogt et al. (1994) and Koeppe et al. (1995) have used deuterium labeling and $^2$H-NMR spectroscopy to accurately define the orientation, mobility, and apparent packing of a palmitoyl chain attached to the gramicidin transmembrane channel. The covalent acyl chain exerts several major molecular changes that we expect to be of general importance for acylated membrane proteins. (1) We observe no long-range, global, or broad effects on conformation that can be ascribed to the covalent acyl chain. (2) The acyl chain greatly slows the motion of the group to which it is attached. For acyl-gA, this group is the ethanolamine tail, while for a palmitoylated membrane protein, this normally would be a cysteine side chain, localized close to the membrane surface (Schmidt, 1989). (3) The acyl chain itself includes both a highly mobile portion, far from its attachment site, and an essentially immobile portion where it is attached to the protein (Vogt et al., 1994). (4) The acyl chain can pack, while retaining its mobility, with rather nice hydrophobic contacts alongside hydrophobic parts of the protein, such as the side chains of Leu, Val, Ile, Trp, and Phe (Figures 6 and 7). (5) A covalent acyl chain will perturb locally the average orientation and probably also the dynamics of selected side chains (Koeppe et al., 1995). (6) Acyl chains may increase the membrane association of proteins and influence the interactions of transmembrane subunits, thereby providing opportunities for the regulation of biological activity. Acylgramicidins therefore have led to some guiding principles concerning covalent lipid−protein interactions.

## ACKNOWLEDGMENT

We thank Jennifer Loukota and Marti Scharlau for assistance with the solid-phase synthesis and Olaf Andersen and Gwendolyn Mattice for helpful discussions.

## REFERENCES

Abdul-Manan, Z., & Hinton, J. F. (1994) *Biochemistry 33*, 6773−6783.
Arsen'ev, A. S., Barsukov, I. L., Bystrov, V. F., Lomize, A. L., & Ovchinnikov, Y. A. (1985) *FEBS Lett. 186*, 168−174.
Arsen'ev, A. S., Lomize, A. L., Barsukov, I. L., & Bystrov, V. F. (1986) *Biol. Membr. 3*, 1077−1104.
Bañó, M. C., Braco, L., & Abad, C. (1992) *Biophys. J. 63*, 70−77.
Becker, M. D., Greathouse, D. V., Koeppe, R. E., II, & Andersen, O. S. (1991) *Biochemistry 30*, 8830−8839.
Bonatti, S., Migliaccio, G., & Simons, K. (1989) *J. Biol. Chem. 264*, 12590−12595.
Cifu, A., Koeppe, R. E., II, & Andersen, O. S. (1992) *Biophys. J. 61*, 189−203.
Cornell, B. A., Separovic, F., Baldassi, A. J., & Smith, R. (1988) *Biophys. J. 53*, 67−76.
Crise, B., & Rose, J. K. (1992) *J. Biol. Chem. 267*, 13593−13597.
Durkin, J. T., Koeppe, R. E., II, & Andersen, O. S. (1990) *J. Mol. Biol. 211*, 221−234.
Durkin, J. T., Providence, L. L., Koeppe, R. E., II, & Andersen, O. S. (1993) *J. Mol. Biol. 231*, 1102−1121.
Etchebest, C., & Pullman, A. (1984) *FEBS Lett. 170*, 191−195.
Etchebest, C., Pullman, A., & Ranganathan, S. (1985) *Biochim. Biophys. Acta 818*, 23−30.
Favre, E., Baroin, A., Bienvenue, A., & Devaux, P. F. (1979) *Biochemistry 18*, 1156−1162.
Greathouse, D. V., Hinton, J. F., Kim, K. S., & Koeppe, R. E., II. (1994) *Biochemistry 33*, 4291−4299.
Hu, W., Lee, K. C., & Cross, T. A. (1993) *Biochemistry 32*, 7035−7047.
Hu, W., Lazo, N. D., & Cross, T. A. (1995) *Biochemistry 34*, 14138−14146.
Jing, S., & Trowbridge, I. S. (1990) *J. Biol. Chem. 265*, 11555−11559.
Ketchem, R. R., Hu, W., & Cross, T. A. (1993) *Science 261*, 1457−1460.
Killian, J. A., Prasad, K. U., Hains, D., & Urry, D. W. (1988) *Biochemistry 27*, 4848−4855.
Killian, J. A., Taylor, M. J., & Koeppe, R. E., II. (1992) *Biochemistry 31*, 11283−11290.
Koeppe, R. E., II, & Weiss, L. B. (1981) *J. Chromatogr. 208*, 414−418.
Koeppe, R. E., II, Paczkowski, J. A., & Whaley, W. L. (1985) *Biochemistry 24*, 2822−2826.
Koeppe, R. E., II, Providence, L. L., Greathouse, D. V., Heitz, F., Trudelle, Y., Purdie, N., & Andersen, O. S. (1992) *Proteins 12*, 49−62.
Koeppe, R. E., II, Killian, J. A., & Greathouse, D. V. (1994a) *Biophys. J. 66*, 14−24.
Koeppe, R. E., II, Greathouse, D. V., Jude, A., Saberwal, G., Providence, L. L., & Andersen, O. S. (1994b) *J. Biol. Chem. 269*, 12567−12576.
Koeppe, R. E., II, Killian, J. A., Vogt, T. C. B., De Kruijff, B., Taylor, M. J., Mattice, G. L., & Greathouse, D. V. (1995) *Biochemistry 34*, 9299−9306.
Lee, K. C., & Cross, T. A. (1994) *Biophys. J. 66*, 1380−1387.
Lee, K. C., Huo, S., & Cross, T. A. (1995) *Biochemistry 34*, 857−867.
Lomize, A. L., Orekhov, V. Y., & Arsen'ev, A. S. (1992) *Bioorg. Khim. 18*, 182−200.
Moench, S. J., Moreland, J., Stewart, D. H., & Dewey, T. G. (1994) *Biochemistry 33*, 5791−5796.
Nicholson, L. K., Moll, F., Mixon, T. E., LoGrasso, P. V., Lay, J. C., & Cross, T. A. (1987) *Biochemistry 26*, 6621−6626.
O'Connell, A. M., Koeppe, R. E., II, & Andersen, O. S. (1990) *Science 250*, 1256−1259.
O'Dowd, B. F., Hnatowich, M., Caron, M. G., Lefkowitz, R. J., & Bouvier, M. (1989) *J. Biol. Chem. 264*, 7564−7569.
Papac, D. L., Thornburg, K. R., Bullesbach, E. E., Crouch, R. K., & Knapp, D. R. (1992) *J. Biol. Chem. 267*, 16889−16894.
Pullman, A. (1987) *Q. Rev. Biophys. 20*, 173−200.
Pullman, A., & Etchebest, C. (1983) *FEBS Lett. 163*, 199−202.
Randall, W. R. (1994) *J. Biol. Chem. 269*, 12367−12374.
Rose, J. K., Adams, G. A., & Gallione, C. J. (1984) *Proc. Natl. Acad. Sci. U.S.A. 81*, 2050−2054.

Schmidt, M. F. G. (1989) *Biochim. Biophys. Acta 988*, 389−411.
Schweizer, A., Rohrer, J., & Kornfeld, S. (1995) *J. Biol. Chem. 270*, 9638−9644.
Smith, R., Thomas, D. E., Atkins, A. R., Separovic, F., & Cornell, B. A. (1990) *Biochim. Biophys. Acta 1026*, 161−166.
Trudelle, Y., Daumas, P., Heitz, F., Etchebest, C., & Pullman, A. (1987) *FEBS Lett. 216*, 11−16.
Veatch, W., & Stryer, L. (1977) *J. Mol. Biol. 113*, 89−102.
Veit, M., & Schmidt, M. F. G. (1993) *FEBS Lett. 336*, 243−247.
Veit, M., Kretzschmar, E., Kazumichi, K., Garten, W., Schmidt, M. F. G., Klenk, H. D., & Roh, R. (1991) *J. Virol. 65*, 2491−2500.
Vogt, T. C. B., Killian, J. A., Demel, R. A., & De Kruijff, B. (1991) *Biochim. Biophys. Acta 1069*, 157−164.
Vogt, T. C. B., Killian, J. A., De Kruijff, B., & Andersen, O. S. (1992) *Biochemistry 31*, 7320−7324.
Vogt, T. C. B., Killian, J. A., & De Kruijff, B. (1994) *Biochemistry 33*, 2063−2070.
Wallace, B. A., Veatch, W. R., & Blout, E. R. (1981) *Biochemistry 20*, 5754−5760.
Wiberg, K. B., & Laidig, K. E. (1987) *J. Am. Chem. Soc. 109*, 5935−5943.
Williams, L. P., Narcessian, E. J., Andersen, O. S., Waller, G. R., Taylor, M. J., Lazenby, J. P., Hinton, J. F., & Koeppe, R. E., II. (1992) *Biochemistry 31*, 7311−7319.
Wilson, P. T., & Bourne, H. R. (1995) *J. Biol. Chem. 270*, 9667−9675.
Zhang, Z., Pascal, S. M., & Cross, T. A. (1992) *Biochemistry 31*, 8822−8828.

BI952046O